(3) The manufacturing and winding of the home-made 7 T superconducting magnet have been finished and the coils have been tested by liquid nitrogen.

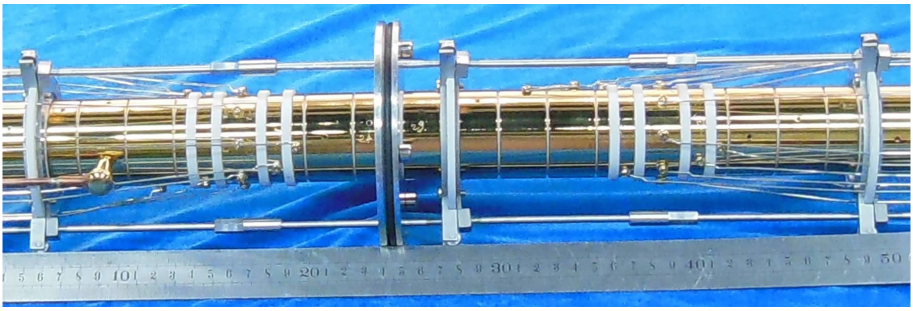

Fig. 1 Photo of the two Penning traps.

2 - 22 Isospin Effect on Transverse Flow for Isobaric Fragments from Nuclear Collisions at Intermediate Energy

Liu Xingquan, Wada Roy, Chen Zhiqiang, Huang Meirong, Lin Weiping
Zhang Suyalatu, Jin Zengxue, Han Rui, Liu Jianli and Shi Fudong

Isospin effects, especially from system isospin asymmetry and fragment isospin asymmetry, are introduced into transverse flow extraction mainly via various physical quantities such as symmetry potential, NN cross section, and coulomb force. Since lots of efforts have been carried out to study the isospin effect by comparing the colliding pairs with different isospin in both experiment[1-5] and theoretical calculations[6-8], in these paper, we focus on the fragment isospin effect on the flow for isobaric fragments.

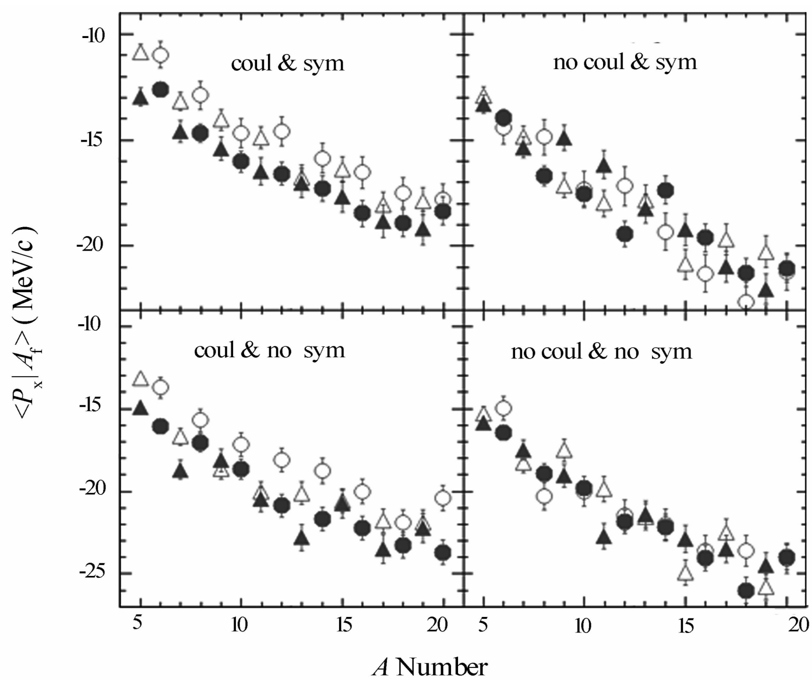

Fig. 1 Transverse flow in the reaction ^{40}Ca + ^{40}Ca at 35 AMeV extracted from different CoMD calculations versus A number. Isobaric fragments with $I(N-Z)=-1-2$ are displayed with △ $I=-1$, ○ $I=0$, ▲ $I=1$, ● $I=2$, respectively.

Transverse flow extracted from primary IMFs(t=300 fm/c) from various CoMD calculations with b=3 fm is compared in Fig. 1. In these calculations, isospin dependent NN cross section remains constant and only the coulomb force and symmetry energy are turned on or turned off to investigate the their contributions in the isospin effect in isolation. Comparing the two columns in Fig. 1, for a given A, larger flow is obtained from isotopes with smaller isospin from the calculation with coulomb: $\mathrm{Flow}_{I=-1}>\mathrm{Flow}_{I=1}$ for odd A isotopes; $\mathrm{Flow}_{I=0}>\mathrm{Flow}_{I=2}$ for even A isotopes. In contrast, without coulomb force, the isospin effect on transverse flow doesn′t show up. Furthermore, even coulomb force is turned off, the transverse flow for isobaric fragments with different I doesn't appear distinguishable in the cases with or without symmetry energy. Additionally, transverse flow for the primary fragments(t=300 fm/c) from AMD calculations is also displayed in Fig. 2. Similar result as the CoMD case is obtained. From these series of comparison, one can qualitatively draw a general conclusion that the coulomb effect contributed in the fragment isospin effect dominates over the symmetry energy effect. Watching from the trend of transverse flow over A in the four plots in Figs. 1 and 2, one can also easily notice an obvious linear increasing trend as A increases. This mass dependence of flow can be also explained as the thermal motion and the limitary of thermal equilibrium, like the charge dependence which has already detailedly introduced in the previous section. When turning off coulomb force and symmetry energy, the linear increasing trend still exists, demonstrating this trend is not attributed to bothcoulomb force and symmetry energy.

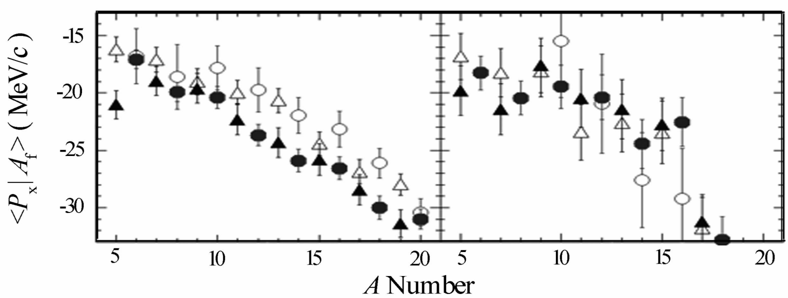

Fig. 2 Transverse flow in the reaction $^{40}Ca+^{40}Ca$ at 35 AMeV extracted from different AMD calculations versus A number. Isobaric fragments with $I(N-Z)=-1-2$ are displayed with △ $I=-1$, ○ $I=0$, ▲ $I=1$, ● $I=2$, respectively.

Figs. 3 and 4 are presented to take a further step to interpret how the coulomb effect causes the isotopes with smaller isospin show a larger transverse flow for a given A. The density and momentum distributions of total nucleons in the phase space are displayed over time in Figs. 3 and 4. Allowing for the symmetry of projectile and target, here only the $Z>0$ and $P_z>0$ side is taken into account. The distributions in both coordinate and momentum space show the projectiles and targets contact at 20～40 fm/c. From 40 to 60 fm/c, compressive nuclear matters are generated and during this time, the momentum is redistributed in the violent competition between attractive interaction produced by mean field and repulsive interaction produced by coulomb force and NN collisions. Due to the dominance of mean field at low incident energies(Here is 35 AMeV), a part of longitudinal momentum transforms into minus transverse, producing negative transverse flow. From 60 to 100 fm/c, complex momentum exchange process keeps driving the system to dynamical equilibrium so that two momentum density centers disappear and a new momentum density center appears at $P_x=P_z=0$. Before 100 fm/c the role of coulomb force is to keep reducing the flow of protons, because it always pushes charge particles to the $P_x>0$ side. However after 100 fm/c, the whole system rotates through $X=0$ in the coordinate space, coulomb force pushes the charge particles to a totally opposite direction, the $P_x<0$ direction. That makes more protons pile up at relative larger P_x region in the momentum space and at the region near PLF or TLF components in the coordinate space. As the time goes on, the density of the overlapped region becomes lower and lower, and the nucleons around the same locations in the phase space tend to bond together. At last the cluster-like structures with a certain isospin and free nucleons are emitted together in the forms of fragments at "freeze-out" time. Thus, for a given A, the IMFs with smaller isospin prefer to having a larger transverse flow. After "freeze-out", the relative density and relative momentum distributions in the phase space don′t charge so much at all.

During the period of expansion, isospin diffusion[9-10] and migration[11-12] also exist, but comparing with these effects, the coulomb effect on the transverse flow is the most dominant(Figs. 1 and 2). Additionally, since the coulomb effect causes the fragment isospin dependence of transverse flow, we can predict the earliest "freeze-out" time is 120 fm/c from AMD calculation at low incident energies and the flow also can't saturate before 120 fm/c, but previous theoretical results have provided the saturation time of transverse flow is much earlier than 100 fm/c[13-16].

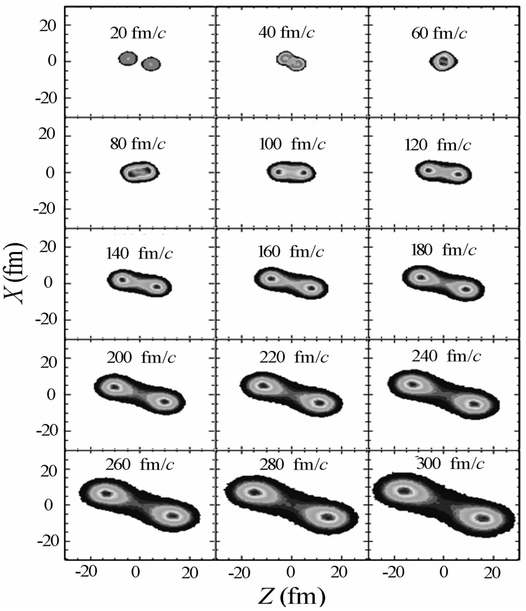

Fig. 3 The total nucleon density evolution in the coordinate space for $^{40}Ca + ^{40}Ca$ at 35 AMeV from AMD calculation.

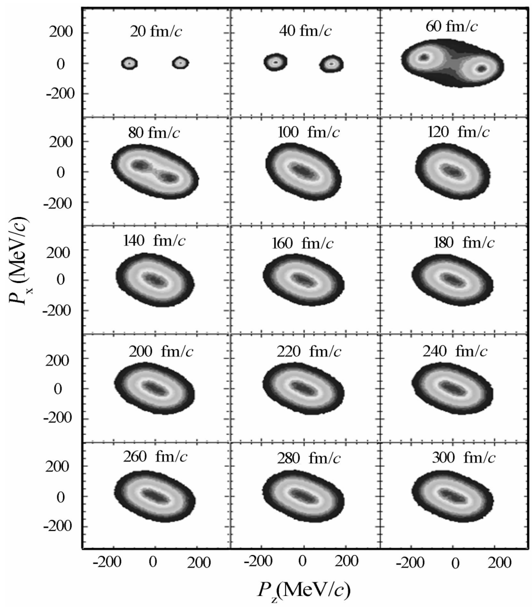

Fig. 4 The total nucleon momentum density evolution in the momentum space for $^{40}Ca + ^{40}Ca$ at 35 AMeV from AMD calculation.

References

[1] R. Pak, et al., Phys. Rev., L78(1997)1022.
[2] R. Pak, et al., Phys. Rev., L78(1997)1026.
[3] Z. Kohley, et al., Phys. Rev., C82(2010)064601.
[4] Z. Kohley, et al., Phys. Rev., C83(2011)044601.
[5] Z. Kohley, et al., Phys. Rev., C85(2012)064605.
[6] B. A. Li, L. W. Chen, C. M. Ko, Phys. Rep., 464(2008)113.
[7] Z. Q. Feng, Phys. Rev., C85(2012)014604.
[8] S. Gautam, et al., Phys. Rev., C86(2012)034607.
[9] M. B. Tsang, et al., Phys. Rev., L92(2004)062701.
[10] T. X. Liu, et al., Phys. Rev., C76(2007)034603.
[11] R. Lionti, et al., Phys. Lett., B625(2005)33.
[12] J. Rizzo, et al., Nucl. Phys., A806(2008)79.
[13] A. Bonasera, et al., Phys. Rep, 243(1994)1.
[14] J. Zhang, et al., Phys. Rev., C50(1994)1617.
[15] R. Nebauer, et al., Nucl. Phys., A650(1999)65.
[16] A. D. Sood, et al., Phys. Rev., C65(2004)054612.